Proceedings of ISINN-29, JINR, E3-2023-58, Dubna, 2023, p.103 –114

On the Significant Enhancement of the Stern-Gerlach Effect for Neutron, Diffracting in a Crystal at Bragg Angles Close to the Right One

V.V. Fedorov, V.V. Voronin, S.Yu. Semenikhin

NRC «Kurchatov Institute» – PNPI, Gatchina, Leningrad reg., Russia

A significant enhancement of any external force acting on a neutron during diffraction at Bragg angles close to $\pi/2$ is discussed for the case of Laue diffraction and detailed description of the effect is given. Such enhancement is due, on the one hand, to the smallness of the Darwin width compared to the Bragg angle, which leads to the well-known diffraction gain of about 10^5, and, on the other hand, to a significant slowing down of the neutron in the crystal at diffraction angles close to the right one, which can give an additional factor about 10^2 or more. Also discussed are the Kato trajectories for a diffracting neutron in a crystal and their "curvature" under the action of an external force. A simple derivation of Kato equations, describing these trajectories is given. As an example of such force we have considered the action on the neutron of a small gradient of the magnetic field. Taking into account the Bormann anomalous absorption effect, it is shown that the Stern–Gerlach effect will be clearly manifested for diffracting neutrons even in a weak magnetic field gradient. The effect amplification factor for a neutron in a crystal (at Bragg angle of 82°) can reach a value of 10^7 compared to a neutron in a "free" space (when the crystal is removed from the setup) in the same field gradient. Experimental results are demonstrated, they are in a good agreement with the theory.

1. In Laue diffraction of X-rays or particles by crystal there is a well-known and unusual amplification effect (see the review by Batterman and Cole [1], for example): small changes (within the Bragg width γ_B) in the angle between the wave vector **k**, of the incident radiation and the system of reflecting planes (i.e., the planes which are near the orientation satisfying the Bragg condition $\lambda = 2d \sin \theta_B$) alter the propagation directions of the rays (Bloch waves) in the crystal over a range θ_B which is much greater than the angle γ_B. The gain factor θ_B/γ_B can reach 10^5–10^6.

Such small deviation from the exact Bragg condition, which leads to significant change in direction of the diffracting ray in crystal, can be caused by a small elastic deformation [2] of the crystal or (for example, for neutrons) by the action of an external force (gravitational or magnetic, for example) [3]. Kato [2] has developed eikonal approach for Bloch waves to describe X-ray diffraction in distorted crystal. In two wave approximation he has got equations for two types of wave packets, propagating in crystal, analogous to those, describing the movement of relativistic “particles” under action of “Kato forces” of opposite direction, which curves the corresponding “Kato trajectories” of these two-wave packets (quasiparticles) in opposite directions. Later Zeilinger et al. [4] have interpreted this in a following way. The quasiparticles, corresponding to different kinds of Bloch waves have "effective masses" of opposite signs, and the enhancement of the external force, acting on neutrons (the large curvature of trajectories) is due to essential decreasing (by about 10^5–10^6 times) the quasiparticle effective masses[1)]. Authors [4] have measured the splitting of those neutron “trajectories” in the perfect crystal in magnetic field gradient. The effects for neutrons from both gravity and crystal deformation were discussed by Sumbaev [5] and measured [6].

Another important feature of Laue diffraction is the possibility of a significant slowing down of the neutron in the crystal by using Bragg angles close to $\pi/2$, since during diffraction the neutron moves on average along the crystallographic planes [7,8]. This velocity component determined by the Bragg angle can be significantly reduced at least by an order of magnitude, compared to the total neutron velocity. Thus, the residence time of the neutron in the crystal determined by namely this velocity component can be significantly increased. This was first noticed in [9] and proposed to be used to increase the effect of the electric dipole moment of a neutron on its diffraction in a non-centrosymmetric crystal. An experimental measurement of the time a neutron spends in crystal was carried out in [10,11].

A significant additional enhancement of the external effect on the diffracting neutron for Bragg angles θ_B close to the right angle was observed in the case of deformation of the crystal by a temperature gradient [12]. The new method to measure a neutron electric charge and the ratio of inertial to gravitational masses has been proposed [13] based on this magnification. The estimations have shown a feasibility to improve the accuracy of a neutron electric charge measurement by about two orders of magnitude in comparison with the current value, and to measure the ratio of inertial to gravitational masses m/m_G with the accuracy $\sim 10^{-6}$.

Here we give a simple derivation of the Kato equations for large Bragg angles using an explicit form of expressions for the neutron probability current density in a crystal (unlike Kato, who obtained his equations based on the dispersion surface equation for X-ray or particle in a crystal, using the normal direction of the energy flow in the crystal to the dispersion surface).

As an example of the mentioned amplification, we will consider the spatial splitting of an unpolarized neutron beam into two polarized beams (with opposite spin directions) during Laue diffraction at large Bragg angles in a crystal located in a small magnetic field gradient (analogous to the Stern–Gerlach effect). Note that, in contrast, the authors [4] observed the splitting of an unpolarized neutron beam into two also unpolarized beams.

2. Next, we will consider diffraction in a symmetrical Laue scheme (the crystal boundary is perpendicular to the reflecting planes, see Fig.1), in an ideal, non-absorbing, thick crystal at large diffraction angles (i.e. close to 90^o).

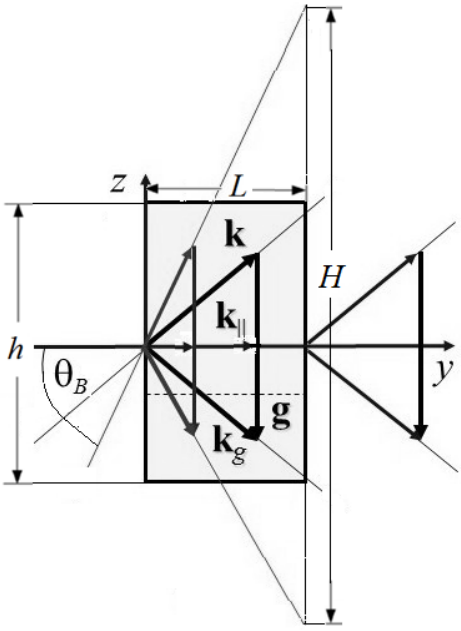

Fig.1. Symmetrical Laue diffraction scheme. L is a crystal thickness, h is its height, H is the length of the Bormann triangle base (shown for large Bragg angle, in this case $H > h$). **g** is a reciprocal lattice vector, characterizing the system of the reflecting planes. Vector **g** is perpendicular to them and its magnitude $g = 2\pi/d$, where d is interplanar distance, **k** is wave vector of the direct neutron wave in the crystal, $\mathbf{k}_g = \mathbf{k} + \mathbf{g}$ is that of the reflected wave. The equality $|\mathbf{k}_g| = |\mathbf{k}|$ is the exact Bragg condition, which is equivalent to the well-known expression $\lambda = 2d \sin\theta_B$.

What do these mean?

1. "Perfect" means that the mosaicity of a crystal much less, than the Bragg (Darwin) diffraction width.
2. "Non-absorbing" means that absorption length is more than the crystal thickness and much more than extinction length.
3. "Thick" means crystal thickness (~ 20 cm in our case) is much more than extinction length.
4. "Large diffraction angles" means $\theta_B = 78^o$–82^o, $\tan\theta_B = 4.7$–7.1 (for example, $\tan 87^o = 19$).

The nuclear potential of the system of reflecting planes **g** responsible to diffraction has the form:

$$V_{\mathbf{g}}(\mathbf{r}) = V_0 + 2V_g \cos \mathbf{gr}, \tag{1}$$

where V_0 is the average nuclear potential of the crystal, V_g is the amplitude of the **g**-harmonic of the periodic crystal potential, which describes the reflecting planes. This potential can only transfer the momenta equal to 0 and $\pm\hbar\mathbf{g}$.

3. Let the neutron beam fall on the crystal at the Bragg angle (see Fig. 1). It is known from the theory of dynamic diffraction (see, for example [1,14]), that two types of Bloch waves $\psi^{(1)}$ and $\psi^{(2)}$ will be exited in the crystal in this case. They are symmetric and antisymmetric:

$$\psi^{(1)} = \frac{1}{\sqrt{2}}\left[e^{i\mathbf{k}^{(1)}\mathbf{r}} + e^{i\left(\mathbf{k}^{(1)}+\mathbf{g}\right)\mathbf{r}}\right] = \sqrt{2}\cos\left(\frac{\mathbf{gr}}{2}\right)e^{\left[i\left(\mathbf{k}^{(1)}+\frac{\mathbf{g}}{2}\right)\mathbf{r}\right]} \equiv \sqrt{2}\cos\left(\frac{\mathbf{gr}}{2}\right)e^{i\mathbf{k}_{\parallel}^{(1)}\mathbf{r}}, \tag{2}$$

$$\psi^{(2)} = \frac{1}{\sqrt{2}}\left[e^{i\mathbf{k}^{(2)}\mathbf{r}} - e^{i\left(\mathbf{k}^{(2)}+\mathbf{g}\right)\mathbf{r}}\right] = -i\sqrt{2}\sin\left(\frac{\mathbf{gr}}{2}\right)e^{i\left(\mathbf{k}^{(2)}+\frac{\mathbf{g}}{2}\right)\mathbf{r}} = -i\sqrt{2}\sin\left(\frac{\mathbf{gr}}{2}\right)e^{i\mathbf{k}_{\parallel}^{(2)}\mathbf{r}}. \tag{3}$$

The wave vectors $\mathbf{k}^{(1)}$ and $\mathbf{k}^{(2)}$ belong to two branches of the dispersion surface:

$$k^{(1,2)2} = K^2 + \Delta_g \mp \sqrt{\Delta_g^2 + \left|U_g\right|^2} \xrightarrow{\Delta_g << U_g} K^2 \mp \left|U_g\right| \tag{4}$$

Here k_0 is the wave vector of the incident neutron, and K is the same vector with the average refractive index of the crystal, taking into account:

$$K^2 \equiv n^2 k_0^2 = k_0^2 - U_0,\ U_{0,g} \equiv 2mV_{0,g}/\hbar^2. \tag{5}$$

The parameter

$$\Delta_g = \left(k_g^2 - k^2\right)/2 \equiv \left[\left(\mathbf{k}+\mathbf{g}\right)^2 - k^2\right]/2 = \left(2\mathbf{kg} - g^2\right)/2 \tag{6}$$

describes the deviation from the exact Bragg condition.

As a result, we see that in the case of $\Delta_g = 0$, neutrons in the states (1) and (2) will propagate in the crystal along the crystallographic planes with the slightly different wave vectors (see Fig. 2)

$$\mathbf{k}_{\parallel}^{(1,2)} = \mathbf{k}^{(1,2)} + \mathbf{g}/2, \tag{7}$$

because neutrons in state (1) are concentrated mainly on nuclear planes (at the maxima of the nuclear potential (1)), and in state (2) they are concentrated between them (at the minima of the nuclear potential).

Indeed,

$$|\psi^{(1)}|^2 = 2\cos^2(\mathbf{gr}/2) = 1+\cos(\mathbf{gr}), \tag{8}$$

$$|\psi^{(2)}|^2 = 2\sin^2(\mathbf{gr}/2) = 1-\cos(\mathbf{gr}). \tag{9}$$

Thus, neutrons in states (1) and (2) move in slightly different potentials and therefore have different kinetic energies (respectively, different values of wave vectors and velocities $\upsilon_{\|}^{(1)} < \upsilon_{\|}^{(2)}$), which reflects the presence of two branches of the dispersion surface of neutron in the crystal. The neutron velocities themselves are approximately equal

$$\upsilon_{\|}^{(1)} \approx \upsilon_{\|}^{(2)} \approx \upsilon_{\|} = \frac{\hbar k_{0\|}}{m} = \upsilon_0 \cos\theta_B \approx \upsilon_0\left(\frac{\pi}{2}-\theta_B\right) << \upsilon_0 \text{ at } \theta_B \approx \frac{\pi}{2}. \tag{10}$$

We pay attention that for Bragg angles, close to the right angle, the velocity component along the planes can be significantly less then the total neutron velocity.

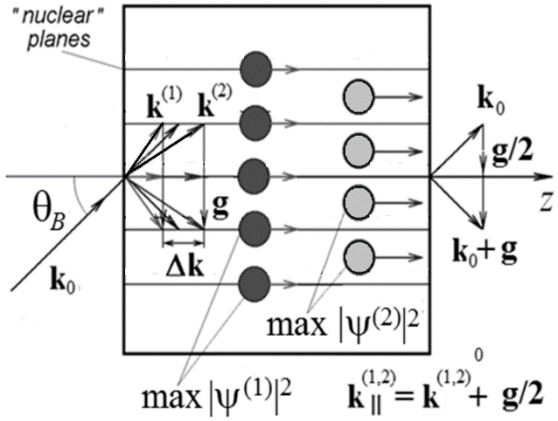

Fig. 2. Symmetrical Laue diffraction scheme. $|\mathbf{k}_g| = |\mathbf{k}|$ (the exact Bragg condition). Neutrons in symmetric (dark circles) and antisymmetric (light circles) states (1) and (2) propagate in the crystal along reflecting nuclear planes with slightly different wave vectors, concentrating on or between the planes.

The difference of wave vectors in a crystal for the exact Bragg condition $\mathbf{k}_0^2 = |\mathbf{k}_0+\mathbf{g}|^2$ is easily calculated, using the equation of the dispersion surface (4):

$$\mathbf{k}^{(2)2} - \mathbf{k}^{(1)2} = 2\mathbf{k}_0\Delta\mathbf{k} = 2k_0\Delta k\cos\theta = 2\left|U_g\right|, \tag{11}$$

and

$$\Delta k = \frac{\left|U_g\right|}{k_0\cos\theta} = \frac{2\left|V_g\right|}{\hbar\upsilon\cos\theta}. \tag{12}$$

Thus, the difference $|\Delta\mathbf{k}|$ contains the angle θ between $\mathbf{k}_0$ and $\Delta\mathbf{k}$. The vector $\Delta\mathbf{k}$ is normal to the crystal boundary, therefore in the case of symmetric Laue diffraction this angle coincides with the Bragg angle: $\theta = \theta_B$.

The interference of waves (1) and (2) in the crystal leads to periodic dependence of the intensities of diffracted beams (direct and reflected) on the thickness of the crystal or the Bragg angle (the so-called Pendellösung fringe). The phase difference that determines these intensity oscillations after passage through a crystal of thickness L is equal to:

$$\Delta\phi = \Delta kL = \frac{\left|U_g\right|L}{k_0\cos\theta_B} = \frac{2\left|V_g\right|}{\hbar}\frac{L}{\upsilon\cos\theta_B}. \tag{13}$$

The value $\xi_g \equiv 2\pi/\Delta k$ is the extinctio the time the neutron s n length. The value $L/\upsilon\cos\theta_B$ in the expression (13) is pends in crystal.

4. The different symmetry of the waves in the crystal leads to another, so called, Bormann effect. This is the effect of abnormal crystal transparency (or abnormal absorption) for waves passing through the crystal under the Bragg conditions. The effect is due to the fact that the wave (1) concentrated on the planes (atoms) is absorbed stronger than the wave (2) concentrated between them.

Neutron absorption in a crystal can be described by adding an imaginary part to the potential ($-iV'$), $V'(\mathbf{r}) <<< V(\mathbf{r})$ is real and positive. It also decomposes into harmonics. As a result, for exact Bragg condition, we will get

$$\mathbf{k}^{(1,2)2} = k_0^2 - U_0 + iU_0' \mp \left(U_g - iU_g'\right) = \mathbf{k}_0^2 - \left(U_0 \pm U_g\right) + i\left(U_0' \pm U_g'\right), \qquad (14)$$

where $U_{0,g}' \equiv 2mV_{0,g}'/\hbar^2, V_{0,g}'$ are corresponding harmonics of an imaginary part of the nuclear potential. So

$$\Delta k^{(1,2)} \equiv \left|\mathbf{k}^{(1,2)} - \mathbf{k}_0\right| = \frac{-\left(U_0 \pm U_g\right) + i\left(U_0' \pm U_g'\right)}{2k_0 \cos\theta_B}, \qquad (15)$$

and Bloch waves (1), (2) will damp with different absorption lengths, so that

$$\left|\psi^{(1,2)}\right|^2 = \left|\psi_0^{(1,2)}\right|^2 e^{-\frac{\left(U_0' \pm U_g'\right)L}{k_0 \cos\theta_B}} \equiv \left|\psi_0^{(1,2)}\right|^2 e^{-\frac{\mu_0\left(1 \pm \varepsilon_g\right)L}{\cos\theta_B}}. \qquad (16)$$

Here

$\varepsilon_g = \dfrac{V_g'}{V_0'}$, $\mu_0 \equiv \dfrac{1}{L_a} = \dfrac{U_0'}{k_0} = k_0 \dfrac{2mV_0'}{\hbar^2 k_0^2}$ is an average damping index, L_a is the corresponding absorption length. For example, for neutrons, moving in silicon (Si), L_a ~ 40 cm. For thermal and cold neutrons in a monoatomic crystal, due to the small size of the nucleus, all harmonics are practically the same, so ε_g can be close to 1. As follows from (16), at sufficiently large Bragg angles, a symmetric Bloch wave can be completely absorbed, while for an antisymmetric wave the crystal will be practically transparent.

5. In the general case $\left(\Delta_g \neq 0\right)$ the neutron wave functions in two wave approximation can be written as

$$\psi^{(1)}(\mathbf{r}) = \cos\gamma e^{i\mathbf{k}^{(1)}\mathbf{r}} + \sin\gamma e^{i\left(\mathbf{k}^{(1)}+\mathbf{g}\right)\mathbf{r}}, \qquad (17)$$

$$\psi^{(2)}(\mathbf{r}) = -\sin\gamma e^{i\mathbf{k}^{(2)}\mathbf{r}} + \cos\gamma e^{i\left(\mathbf{k}^{(2)}+\mathbf{g}\right)\mathbf{r}}. \qquad (18)$$

Here

$\tan 2\gamma = \dfrac{U_g}{\Delta_g} \equiv \dfrac{1}{w_g}$, $w_g = \dfrac{\Delta_g}{U_g} = \dfrac{\left(k_g^2 - k^2\right)}{2U_g} = \dfrac{\left(2\mathbf{kg} + g^2\right)}{2U_g}$ is the dimensionless parameter of the deviation from the exact Bragg condition, so we have

$$\sin^2\gamma = \frac{1}{2}\left[1 - \frac{w_g}{\sqrt{1+w_g^2}}\right], \qquad \cos^2\gamma = \frac{1}{2}\left[1 + \frac{w_g}{\sqrt{1+w_g^2}}\right]. \qquad (19)$$

Averaging over fast oscillations with the period *d* the expression for the current density

$$\mathbf{j}^{(1,2)} = \frac{\hbar}{2mi}\left(\psi^{(1,2)*}\nabla\psi^{(1,2)} - \psi^{(1,2)}\nabla\psi^{(1,2)*}\right) = \frac{\hbar}{m}\,\mathrm{Im}\;\psi^{(1,2)*}\nabla\psi^{(1,2)}, \tag{20}$$

we get for two kinds of waves

$$\mathbf{j}^{(1)} = \frac{\hbar}{m}\left[\,\mathbf{k}^{(1)}\cos^2\gamma + \left(\mathbf{k}^{(1)}+\mathbf{g}\right)\sin^2\gamma\,\right] = \frac{\hbar}{m}\left[\left(\mathbf{k}^{(1)}+\frac{\mathbf{g}}{2}\right) - \frac{\mathbf{g}}{2}\frac{w_g}{\sqrt{1+w_g^2}}\right], \tag{21}$$

$$\mathbf{j}^{(2)} = \frac{\hbar}{m}\left[\,\mathbf{k}^{(2)}\sin^2\gamma + \left(\mathbf{k}^{(2)}+\mathbf{g}\right)\cos^2\gamma\,\right] = \frac{\hbar}{m}\left[\left(\mathbf{k}^{(2)}+\frac{\mathbf{g}}{2}\right) + \frac{\mathbf{g}}{2}\frac{w_g}{\sqrt{1+w_g^2}}\right]. \tag{22}$$

At the exact Bragg condition (w_g= 0) the neutron current densities $\mathbf{j}^{(1)}$ and $\mathbf{j}^{(2)}$ are parallel to the planes (*z* axis in Fig. 3) , so waves (1) and (2) will move along the planes in the crystal.

If $w_g \neq 0$, then the neutron currents (1) and (2) will diverge in opposite directions (Fig. 3).

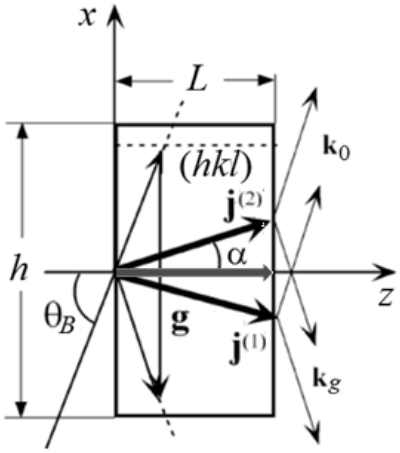

Fig. 3. The bold horizontal arrow gives the directions of the neutron current densities $\mathbf{j}^{(1)}$ and $\mathbf{j}^{(2)}$ for the exact Bragg condition w_g= 0. If $w_g \neq 0$, then the neutron currents $\mathbf{j}^{(1)}$ and $\mathbf{j}^{(2)}$ are deflected by an angle α in the opposite direction.

Kato trajectories are defined as the lines tangent to which coincide with the directions of the current density at each point. In the case of undeformed crystal and absence of the external forces, they are straight lines as shown in Fig. 3. If neutrons fall on the crystal with a small deviation from the Bragg angle, they diverge in opposite directions.

If the incident wave is a wave packet limited, for example, by an entrance slit, then the Kato trajectory will describe the movement of this packet in the crystal (this is correct, if the size of such two waves packet (slit width) is significantly larger than the extinction length).

If $w_g \neq 0$, then the neutron currents (1) and (2) will diverge, so that for a certain thickness of the crystal and finite width of the packets they cease to overlap and will reach the exit surface of the crystal in different points (Fig. 3.).

If deviation from the Bragg angle is small (within the Bragg width, that is $w_g << 1$), then $\mathbf{j}^{(1)}$ and $\mathbf{j}^{(2)}$ will have a simple form:

$$\mathbf{j}^{(1,2)} \approx \frac{\mathrm{h}}{m}\left[\,\mathbf{k}_{\parallel}^{(1,2)} \pm \frac{\mathbf{g}}{2}\frac{\Delta_g}{|U_g|}\right] \equiv \frac{\mathrm{h}}{m}\left[\,\mathbf{k}_{\parallel}^{(1,2)} \pm w_g\,\frac{\mathbf{g}}{2}\right]. \tag{23}$$

Note that $g / 2k_{\mathrm{P}}^{(1,2)} \approx \tan\theta_B$, so the angles α of the slopes of the Kato trajectories for neutrons in states (1) and (2) are determined by $\tan\alpha = \mp w_g \tan\theta_{\mathrm{B}}$.

Also, it is important that in the symmetric Laue scheme waves $\psi^{(1)}$ and $\psi^{(2)}$ (see (17) and (18)) are excited in the crystal with the amplitudes, respectively, cos γ and –sin γ (see [14], for example). Therefore, for small deviations from the Bragg condition, i.e. for w_g<<1 the both states are excited in the crystal with almost the same probability 1/2, because

$$\cos^2\gamma = \frac{1}{2}\left(1+w_g\right) \approx \frac{1}{2}, \text{ and } \sin^2\gamma = \frac{1}{2}\left(1-w_g\right) \approx \frac{1}{2}.$$

However, at the same time, the directions of the currents (especially at Bragg angles θ_B close to 90°, when $k_{\|} << g/2$ and so $\tan\theta_B = g/2k_{\|} >>1$) can change very significantly, see (23). As we already have mentioned, the slopes of the Kato trajectories are determined by

$$\frac{dx}{dz} = \tan\alpha \approx \mp w_g \tan\theta_B, \tag{24}$$

from where follows

$$w_g \approx \frac{\tan\alpha}{\tan\theta_B} \equiv \frac{L\tan\alpha}{L\tan\theta_B}. \tag{25}$$

We see, that the deviation parameter has a simple meaning of the ratio of the coordinate $x = L\tan\alpha$ of the exit point of the Kato trajectory from the crystal to half the length of the base of the Bormann triangle (fan) $L\tan\theta_B$ (see Fig. 1, Fig. 3).

6. Thus, at diffraction angles close to 90°, even a small change in the parameter w_g will lead to a significant change in the direction of the neutron current. If an external force acts on the neutron, the parameter w_g will constantly change, so the trajectories will be curved, and for different types of Bloch waves they will diverge in opposite directions.

The change in the slope of the $x(z)$ curve, describing the Kato trajectory, will be determined by the expression

$$\frac{d^2x}{dz^2} = \mp\tan\theta_B \frac{dw_g}{dz} = \mp\frac{c_0}{\upsilon_{\|}}\frac{dw_g}{dt} \quad \left(c_0 \equiv \tan\theta_B\right). \tag{26}$$

Consider the action of a constant external force **F** on a neutron in a perfect undeformed crystal. Only the force component F_x along the vector **g** (x axis) leads to a change in the deviation parameter w_g. The force components parallel to the planes (along the y and z axes) do not change it. In this case the derivative of w_g is easily calculated

$$\frac{dw_g}{dt} = \frac{d}{dt}\frac{\left(2\mathbf{kg}+g^2\right)}{2U_g} = \frac{gdk_x}{U_g dt} = \frac{2m_n\upsilon_{\perp}}{\hbar^2 U_g}F_x = \frac{\upsilon_{\perp}}{V_g}F_x. \tag{27}$$

Here we used

$$\upsilon_{\perp} \equiv \frac{\hbar g}{2m_n} \ \left(\upsilon_{\perp} \approx \upsilon_{0x}, \upsilon_{\|} = \upsilon_{0z}, \upsilon_{\|} << \upsilon_{\perp}\right), \quad \frac{dk_x}{dt} \equiv \frac{m_n}{\hbar}\frac{d\upsilon_x}{dt} = \frac{F_x}{\hbar}.$$

Finally, the equation for Kato trajectories will be

$$\frac{d^2x}{dz^2} = \mp\frac{c_0}{\upsilon_{\|}}\frac{\upsilon_{\perp}}{V_g}F_x = \mp c_0^2\frac{F_x}{V_g} \equiv \mp c_0^2\frac{E_n}{V_g}\frac{F_{\perp}}{E_n}, \tag{28}$$

where $\upsilon_{\perp}/\upsilon_{\|} = c_0$, $F_x \equiv F_{\perp}$.

The classical Newton's equation for the neutron trajectory in the vacuum under the action of an external force $F_\perp$ directed perpendicular to its velocity is

$$m_n v^2 \frac{d^2x}{dz^2} = F_\perp, \quad \text{that is} \quad \frac{d^2x}{dz^2} = \frac{F_\perp}{2E_n}. \tag{29}$$

Thus, the equation for Kato trajectories can be rewritten as

$$\frac{d^2x}{dz^2} = \mp K_D \frac{F_\perp}{E_n}, \quad K_D = \frac{2c_0^2 E_n}{V_g} \equiv K_{0D} \tan^2 \theta_B. \tag{30}$$

Here $K_{0D} = 2E_n/V_g$ is the usual well known coefficient of the diffraction enhancement, $\tan^2 \theta_B$ describes an additional essential enhancement of the force action, it is associated with an increase of time the neutron spends in the crystal. We see that the effect of the force, due to diffraction in crystal, is increased many times compared to the "empty" space, and the total coefficient of such diffraction enhancement is K_D.

For example, for a system of planes (220) of a silicon crystal with an interplane distance d = 1.92 Å, which is often used in diffraction experiments with neutrons ($E_n = 5.5 \cdot 10^{-3}$ eV, $V_g = 5.2 \cdot 10^{-8}$ eV) the value of the total diffraction gain is:

$$K_{D(\mathrm{Si})}^{220} = 2.1 \cdot 10^5 \tan^2 \theta_B. \tag{31}$$

Already at the Bragg angle $\theta_B \sim 82^\circ$ ($c_0 = 7.1$) the value of K_D is ~ 10^7. For $\theta_B \sim 88^\circ$ ($c_0 \sim 30$) it will be ~ $2 \cdot 10^8$, that is 3 orders more than the usual diffraction enhancement coefficient.

7. Experiment on observation of diffraction enhancement of the Stern–Gerlach effect for neutron was carried out [15,16] at the PF1B neutron beam of the ILL high flux reactor (Grenoble, France). Neutrons were deflected in a small gradient of the magnetic field. In an inhomogeneous magnetic field inside the crystal, forces of opposite direction will act on the neutrons with opposite spin projections (along and against the field) (as in the Stern–Gerlach experiment). Only the force components perpendicular to the planes along the vector **g** (x axis) lead to a change in the direction of the Kato trajectory:

$$F_\perp^{(\pm)} = \mp \mu_n \frac{\partial B}{\partial x} \approx \mp 6 \cdot 10^{-12} \left[\frac{\mathrm{eV}}{\mathrm{G}}\right] \frac{\partial B}{\partial x} \left[\frac{\mathrm{G}}{\mathrm{cm}}\right] \equiv \mp F_w. \tag{32}$$

In our case $\partial B / \partial x \approx 3$ G/cm, so $F_w \sim 2 \cdot 10^{-11}$eV/cm.

The schematic diagram of the experiment is shown in Fig. 4. Two identical crystals are placed in an inhomogeneous magnetic field (Fig. 5). More detailed description see [15,16].

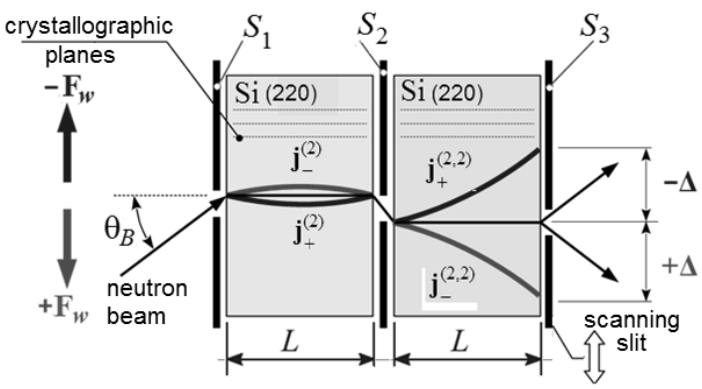

Fig. 4. A double crystal scheme of Laue diffraction with direct neutron beam collimation. $\pm\mathbf{F}_w$ are forces acting on different components (along and against the direction of the magnetic field gradient) of the neutron spin. S_1, S_2 are collimating slits, S_3 is scanning slit, $\pm\Delta$ are displacements of the scanning slit for neutron registration. Kato trajectories for different spin projections are shown in both silicon (Si) crystals.

Nonpolarized neutron beam with a monochromaticity of $\Delta\lambda/\lambda \sim 10^{-2}$ after the monochromator (neutron wave length can be tuned within a range of λ = (3.5–3.9) Å) is impinging the entry face of the probing silicon crystal having dimensions of 130×130×218 mm^3. In the experiment the (220) diffraction planes with an interplane spacing of d = 1.92Å were used. The maximum variation of lattice spacing over the entire crystal volume is in the order of $\Delta d/d \sim 10^{-7}$. To obtain a two-crystal geometry, the Si crystal has a cut in the middle with a depth of 72 mm and a width of 1.6 mm, see Fig. 6.

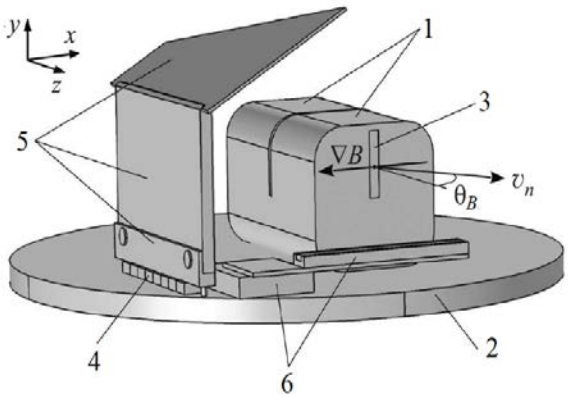

Fig. 5. The design of a magnetic system for creating a magnetic field gradient in a crystal. 1 – silicon crystal, 2 – rotation stage (also part of field guide), 3 – neutron beam exit area, 4 – permanent magnets, 5 – magnetic field guide, 6 – piezo motor for exit slit S_3.

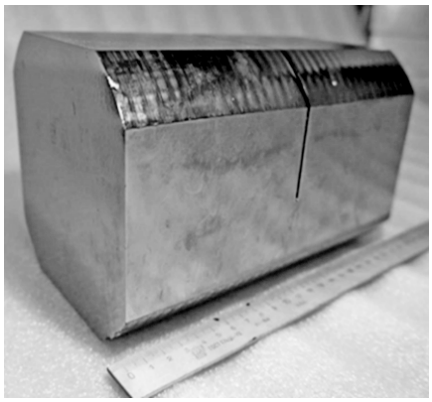

Fig. 6. Silicon probing crystal.

Note, that in our case (large crystal thickness and Bragg angle, i.e. $L_{\text{eff}} = L \tan\theta_B >> L_a$, in both crystals only antisymmetric weakly absorbed waves (2) for both spins "survive". The corresponding Kato trajectories will deviate in different directions (see Fig. 4).

The slits S_1 and S_2 (at x = 0) separate in the first crystal the trajectories of neutrons, which bent in a certain way under the action of forces (set the initial slopes for 2 spin projections). In the absence of forces, these would be trajectories with zero inclination (parallel to the planes, i.e. the z axis) of neutrons falling on the crystal exactly at the Bragg angle.

The presence of an external force will bend these trajectories, so only neutrons falling on the first crystal with fixed (opposite for opposite spins) parameters of deviation can pass through the second slit.

Thus, these slits determine the initial angles of inclination of the trajectories $\pm\alpha_0$. They can be found from the trajectory equations (30) with the boundary condition $x(0) = x(L) = 0$. As a result, in the first crystal these trajectories corresponding to neutrons with opposite polarizations will be described by the curves

$$x^{\pm}(z) = \pm\frac{c_0^2 F_w}{2V_g}(L - z)\,z. \tag{33}$$

In the second crystal, these trajectories will start at opposite angles of inclination, so that the forces will continue to bend them in the same direction ($z' = z - L$):

$$x^{\pm}(z') = \pm\frac{c_0^2 F_w}{2V_g}(L + z')\,z'. \tag{34}$$

As a result, on the exit face of the second crystal, the trajectories of neutrons with different polarizations will shift to

$$x^{\pm}(2L) = \pm\frac{c_0^2 F_w}{V_g} L^2, \tag{35}$$

so, in such a scheme with direct collimation of the beam, the effect of two crystals (of thickness L) doubles (the effect for one crystal in the case of doubling its thickness is quadrupled). The distance between the trajectories at the exit face of the second crystal (splitting) will be equal to

$$\Delta_{2L} = \frac{2c_0^2 F_w}{V_g} L^2 \equiv \frac{4c_0^2 E_n}{V_g}\frac{F_w}{2E_n} L^2 = 2K_D \frac{F_w}{2E_n} L^2. \tag{36}$$

Note that the sensitivity of this experiment to external force acting on a neutron in a crystal is determined by the magnitude of the force F_w required to shift the neutron beam at the exit from the second crystal by the width of the third slit δ_{S3}:

$$F_\delta = \frac{V_g}{2c_0^2 E_n}\frac{2E_n}{L^2}\delta_{S3} = \frac{1}{K_D}\frac{2E_n}{L^2}\delta_{S3}. \tag{37}$$

Here K_D is the diffraction gain coefficient, the value $(2E_n\,\delta_{S3})/L^2$ is the force perpendicular to the direction of motion of the neutron and necessary for its displacement by δ_{S3} in vacuum. We noted already that $K^{220}_{D(\mathrm{Si})} = 2\cdot 10^5 \tan^2\theta_B$, which can reach ~$10^7$ for Bragg angle of 82°.

Measurements [15,16] were carried out for Bragg angles θ_B from 78° to 82°. The minimum sizes of collimating slits (δ_{S1}= 17 mm, δ_{S2} = 15 mm, δ_{S3} = 18 mm) were selected to obtain sufficient statistical accuracy during a limited time of the experiment.

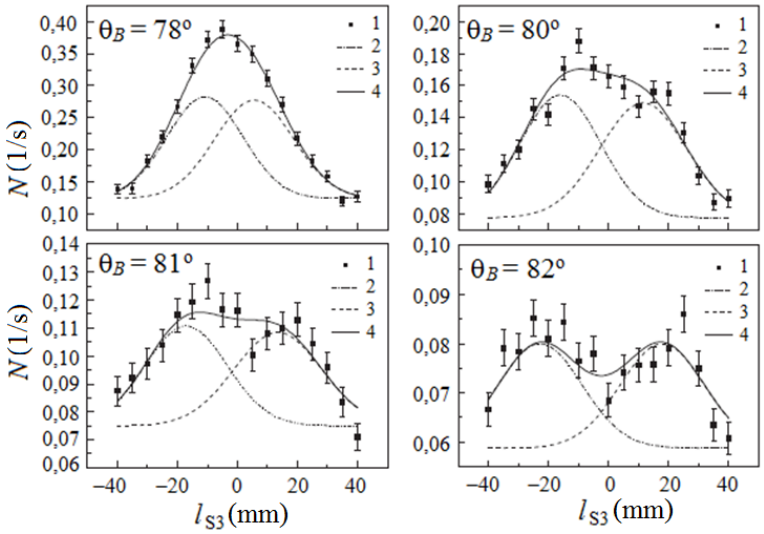

Fig. 7. Intensity distributions at the exit of the probing crystal for a maximum field gradient in the vicinity of the neutron beam for different angles $\theta_B = (78-82)^\circ$ (l_{S3} is the position of the scanning slit S_3).

At a maximum angle of 82°, the splitting value is $\Delta_{\mathrm{exp}} = (4.1 \pm 0.1)$ cm. Using the data from Fig. 7, and expr. (36) we can extract the value of the field gradient (open circles in Fig. 8):

$$\nabla B \equiv \frac{\partial B}{\partial x} = \frac{E_n}{\mu_n K^{220}_{D(\mathrm{Si})} L^2}\Delta_{\mathrm{exp}}. \tag{38}$$

The average value of the magnetic field gradient over the neutron beam in the experiment turned out to be $\nabla B_{\mathrm{av}} = (3.12 \pm 0.09)$ G/cm, which is consistent with estimates based on

magnetometer readings at three points on each side (entrance and exit) of the crystal, which gave the value (3.0 ± 0.3) G/cm, see [17].

The calculation of the spatial splitting of a neutron beam with a wavelength λ = 3.8 Å, $E_n \approx 5.5$ meV (which corresponds to $\theta_B = 82°$), in free space when passing the same distance (21.8 cm) in the same magnetic field gradient through the same 3-slit collimator, but without a crystal (removed from the installation) gives $3.9 \cdot 10^{-7}$ cm. To split by 4.1 cm, the beam must travel ~ 900 m!

Thus, the experimentally measured coefficient of diffraction enhancement is equal $K^{220}_{D(\mathrm{Si})\mathrm{exp}} \approx 2.1 \cdot 10^5 \tan^2\theta_B \approx 1.05 \cdot 10^7$, at $\theta_B = 82°$, which is in good agreement with the theory.

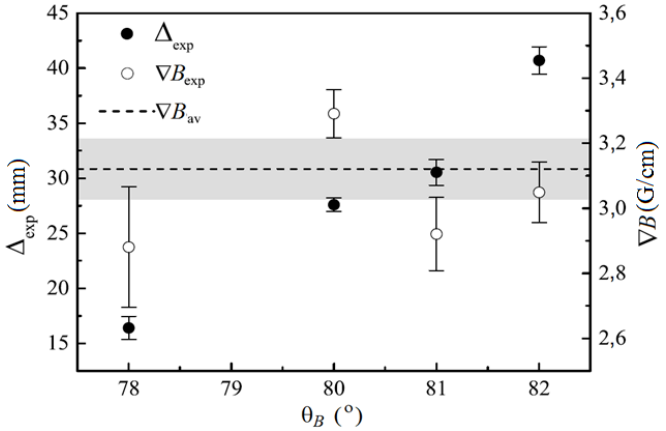

Fig. 8. The dependences of the distance Δ_{exp} between the intensity maxima for two spin projections (Fig. 7) and the field gradient on the Bragg angle. Dotted line is the average value of the magnetic field gradient.

8. Based on the count rates in this experiment [15,16], it is possible to estimate its sensitivity (the error in measuring the external force) achieved per day:

$$\sigma\left(F_{\mathrm{ext}}\right) \approx 2 \cdot 10^{-12} \frac{\mathrm{eV}}{\mathrm{cm} \cdot \mathrm{day}} = 2 \cdot 10^{-3} m g_E \frac{1}{\mathrm{day}}, \tag{39}$$

where g_E is the acceleration of gravity near the Earth's surface. The use of cold neutron sources, such as the planned for PIK reactor with a spectral neutron flux density of ~ $5 \cdot 10^8$ n/Å·cm^2·c, makes it possible to use slits ~ 0.1 mm in size and Bragg angles up to 88^o , while the neutron count rate from one exit slit can reach 50 n/s, which results in an improvement in sensitivity by about 12 000 times. An additional increase in sensitivity by an order of magnitude, for example, can be obtained by using a multi-slit (100 slits) version of the installation. Thus, in principle, sensitivity can reach the level:

$$\sigma\left(F_{\mathrm{ext}}\right) \approx 1.7 \cdot 10^{-17} \frac{\mathrm{eV}}{\mathrm{cm} \cdot \mathrm{day}} = 1.7 \cdot 10^{-8} m g_E \frac{1}{\mathrm{day}}. \tag{40}$$

The attraction force of a neutron by the Sun in the Earth's orbit is

$$F_{GS} = G \frac{m_G M_S}{R_{\mathrm{O}}^2} = 6 \cdot 10^{-13} \mathrm{eV/cm} \approx 6 \cdot 10^{-4} m g_E, \tag{41}$$

where m_G and M_S are the gravitational masses of the neutron and Sun, R_{O} is the radius of the Earth's orbit around the Sun (m is the inertial mass of neutron).

So, there is a good possible application of such installation to measuring the ratio of the inertial and gravitational masses of the neutron. With the sensitivity (40) for 100 days of measurements, one can obtain an error in measuring the ratio m/m_G, better than the current value [17], approximately by two orders of magnitude, more detailed see [18].

Footnote

[1)] The fact itself that an electron in a crystal has effective masses of opposite signs near the boundaries of Brillouin zones, where its dispersion curve has gaps, is well known, see, for example the textbook by G.S. Zhdanov "Solid state physics". Moscow University Press, 1962 (in Russian).

References

1. Batterman B.W., Cole H. Dynamical diffraction of X-ray by perfect crystals. Rev. Mod. Phys., 1964, **36**, 681–717.
2. Kato N. Pendellösung fringe in distorted crystals.
   I. Fermat's principle for Bloch waves. J. Phys. Soc. Jap., 1964, **18**, 1785–1791;
   II. Application to two beam cases. J. Phys. Soc. Jap., 1964, **19**, 67–77;
   III. Application to homogeneously bend crystals. J. Phys. Soc. Jap., 1964, **19**, 971–985.
3. Werner S.A. Gravitational and magnetic field effects on the dynamical diffraction of neutrons. Phys. Rev., 1980, **B 21**, 1774–1789.
4. Zeilinger A., Shull C.G., Horne M.A., Finkelstein K.D. Effective mass of neutrons diffracting in crystals. Phys. Rev. Lett., 1986, **57**, 3089–3092.
5. Sumbaev O.I. Interference effects due to gravity a magnetic field gradient or Earth's rotation in neutron diffraction by an elastically bent single crystal. Preprint LIYaF-676, Leningrad, 1981, 13p.
6. Alekseev V.L., Lapin E.G., Leushkin E.K., Rumyantsev V.L., Sumbaev O.I., Fedorov V.V. Gravitational effect in neutron diffraction by a curved quartz single crystal. Sov. Phys. JETP, 1988, **67** (8), 1727–1733,
7. Fedorov V.V., Smirnov A.I. Properties of electromagnetic radiation emitted by an electron diffracted in a single crystal. Sov. Phys. JETP, 1974, **39**, No.2, 271–274.
8. Shull C.G., Zeilinger A., Squires G.L., Horne M.A., Atwood D.K., Arthur J. Anomalous flight time of neutrons through diffracting crystals. Phys. Rev. Lett., 1980, **44**, 1715–1718.
9. Fedorov V.V., Voronin V.V., Lapin E.G. On the search for neutron EDM using Laue diffraction by a crystal without a centre of symmetry. Preprint LNPI-644. Leningrad,1990, 36 p; J. Phys.,1992, **G 18**, 1133–1148.
10. Voronin V.V., Lapin E.G., Semenikhin S.Yu., Fedorov V.V. Direct measurement of the delay time for a neutron in a crystal in the case of the Laue diffraction. JETP Lett., 2000, **71**, 76–79.
11. Fedorov V.V., Lapin E.G., Semenikhin S.Yu., Voronin V.V. First observation of new effects at the set-up for searching for a neutron electric dipole moment by a crystal-diffraction method. Appl. Phys., 2002, **A 74**, Suppl. 1, 298–301.
12. Fedorov V.V., Kuznetsov I.A., Lapin E.G., Semenikhin S.Yu., Voronin V.V. Neutron Laue diffraction in a weakly deformed crystal at the Bragg angles close to $\pi/2$. JETP Lett., 2007, **85**, No.1, 82–85.
13. Fedorov V.V., Kuznetsov I.A., Lapin E.G., Semenikhin S.Yu., Voronin V.V. Diffraction enhancement and new way to measure neutron electric charge and the ratio of inertial to gravitational mass. Nucl. Instr. Meth., 2008, **A593**, 505–509.
14. P.B. Hirsch, A. Howie, R.B. Nicholson, D.W. Pashley, M.J. Whelan (Eds.), Electron Microscopy of Thin Crystals, Plenum, New York, 1965.
15. Voronin V.V., Semenikhin S.Yu., Shapiro D.D., Braginets Yu.P., Fedorov V.V., Nesvizhevsky V.V., Jentschel M., Ioffe A., Berdnikov Ya.A. Diffraction enhancement of the Stern–Gerlach effect for a neutron in a crystal. JETP Lett., 2019, **110**, No. 9, 581–584.
16. Voronin V.V., Semenikhin S.Yu., Shapiro D.D., Braginets Yu.P., Fedorov V.V., Nesvizhevsky V.V., Jentschel M., Ioffe A., Berdnikov. Ya.A. 7-order enhancement of the Stern-Gerlach effect of neutrons diffracting in a crystal. Phys. Lett, 2020, **B 809**, 135739.
17. Schmiedmayer J. The equivalence of the gravitational and inertial mass of the neutron. Nucl. Instr. Meth., 1989, **A 284**, 59–62.
18. Voronin V.V., Kuznetsov I.A., Lapin E.G., Semenikhin S.Yu., Fedorov V.V. Diffraction enhancement effect and new possibilities of measuring the electric charge of the neutron and its inertial-to-gravitational mass ratio. Phys. Atom. Nucl., 2009, **72**, No. 3, 470–476.